

## Research Article

# SmartMIMO: An Energy-Aware Adaptive MIMO-OFDM Radio Link Control for Next-Generation Wireless Local Area Networks

Bruno Bougard,<sup>1,2</sup> Gregory Lenoir,<sup>1</sup> Antoine Dejonghe,<sup>1</sup> Liesbet Van der Perre,<sup>1</sup> Francky Catthoor,<sup>1,2</sup> and Wim Dehaene<sup>2</sup>

<sup>1</sup>IMEC, Department of Nomadic Embedded Systems, Kapeldreef 75, 3001 Leuven, Belgium

<sup>2</sup>K. U. Leuven, Department of Electrical Engineering, Katholieke Universiteit Leuven, ESAT, 3000 Leuven, Belgium

Received 15 November 2006; Revised 12 June 2007; Accepted 8 October 2007

Recommended by Monica Navarro

Multiantenna systems and more particularly those operating on multiple input and multiple output (MIMO) channels are currently a must to improve wireless links spectrum efficiency and/or robustness. There exists a fundamental tradeoff between potential spectrum efficiency and robustness increase. However, multiantenna techniques also come with an overhead in silicon implementation area and power consumption due, at least, to the duplication of part of the transmitter and receiver radio front-ends. Although the area overhead may be acceptable in view of the performance improvement, low power consumption must be preserved for integration in nomadic devices. In this case, it is the tradeoff between performance (e.g., the net throughput on top of the medium access control layer) and average power consumption that really matters. It has been shown that adaptive schemes were mandatory to avoid that multiantenna techniques hamper this system tradeoff. In this paper, we derive *smartMIMO*: an adaptive multiantenna approach which, next to simply adapting the modulation and code rate as traditionally considered, decides packet-per-packet, depending on the MIMO channel state, to use either space-division multiplexing (increasing spectrum efficiency), space-time coding (increasing robustness), or to stick to single-antenna transmission. Contrarily to many of such adaptive schemes, the focus is set on using multiantenna transmission to improve the link energy efficiency in real operation conditions. Based on a model calibrated on an existing reconfigurable multiantenna transceiver setup, the link energy efficiency with the proposed scheme is shown to be improved by up to 30% when compared to nonadaptive schemes. The average throughput is, on the other hand, improved by up to 50% when compared to single-antenna transmission.

Copyright © 2007 Bruno Bougard et al. This is an open access article distributed under the Creative Commons Attribution License, which permits unrestricted use, distribution, and reproduction in any medium, provided the original work is properly cited.

## 1. INTRODUCTION

The performance of wireless communication systems can drastically be improved when using multiantenna transmission techniques. Specifically, multiantenna techniques can be used to increase antenna gain and directionality (beamforming, [1]), to improve link robustness (space-time coding [2, 3]), or to improve spectrum efficiency (space division multiplexing [4]). Techniques where multiple antennas are considered both at transmit and receive sides can combine those assets and are referred to as multiple-input multiple-output (MIMO). On the other hand, because of its robustness in harsh frequency selective channel combined with a low implementation cost, orthogonal frequency division multiplexing (OFDM) is now pervasive in broadband wireless communication. Therefore, MIMO-OFDM schemes turn out to be excellent candidates for next generation broadband wireless standards.

Traditionally, the benefit of MIMO schemes is characterized in terms of *multiplexing gain* (i.e., the increase in spectrum efficiency) and *diversity gain* (namely, the increase in immunity to the channel variation, quantified as the order of the decay of the bit-error rate as a function of the signal-to-noise ratio). In [5], it is shown that, given a multiple-input multiple-output (MIMO) channel and assuming a high signal-to-noise ratio, there exists a fundamental tradeoff between how much of these gains a given coding scheme can extract. Since then, the merit of a new multiantenna scheme is mostly evaluated with regard to that tradeoff. However, from the system perspective, one has also to consider the impact on implementation cost such as silicon area and energy efficiency. When multiantenna techniques are integrated in battery-powered nomadic devices, as it is mostly the case for wireless systems, it is the tradeoff between the effective link performance (namely, the net data rate on top of the medium access control layer) and the link energy efficiency

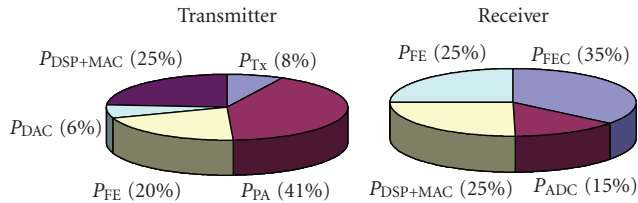


FIGURE 1: Power consumption breakdown of typical single-antenna OFDM transceivers [6, 7]. At the transmit part, the power amplifier contribution ( $P_{TX} + P_{PA}$ ), which can scale with the transmit power and linearity if specific architectures are considered [8], accounts for 49%. At the receiver, the digital baseband processing ( $P_{DSP}$ ), forward error correction ( $P_{FEC}$ ), and medium access control ( $P_{MAC}$ ) units are dominant and do not scale with the transmit power. The power of the analog/digital and digital/analog converters ( $P_{ADC} + P_{DAC}$ ) and the fixed front-end power ( $P_{FE}$ ) are not considered because they are constant.

(total energy spent in the transmission and the reception per bit of data) that really matter. Characterizing how a diversity gain, a multiplexing gain, and/or a coding gain influence that system-level tradeoff remains a research issue.

The transceiver power consumption is generally made of two terms. The first corresponds to the power amplifier(s) consumption and is a function of the transmit power, inferred from the link budget. The second corresponds to the other electronics consumption and is independent of the link budget. We refer, respectively, to dynamic and static power consumption. The relative contribution of those terms is illustrated in Figure 1 where the typical power consumption breakdown of single-antenna OFDM transceivers is depicted.

The impact on power consumption of multiantenna transmission (MIMO), when compared with traditional single-antenna transmission (SISO), is twofold. On the one hand, the general benefit in spectral efficiency versus signal-to-noise ratio can be exploited either to reduce the required transmit power, with impact on the dynamic power consumption, or to reduce the transceiver duty cycle with impact on both dynamic and static power contributions. On the other hand, the presence of multiple antennas requires duplicating part of the transceiver circuitry, which increases both the static and dynamic terms.

The question whether multiantenna transmission techniques increase or decrease the transceiver energy efficiency has only recently been addressed in the literature [9–11]. Interestingly, it has been shown that for narrow-band single-carrier transmission, multiantenna techniques basically decrease the energy efficiency if they are not combined with adaptive modulation [9]. It has also been shown, in the same context, that energy efficiency improvement is achievable by adapting the type of multiantenna encoding to the transmission condition [10, 11].

The purpose of this paper is first to extend previously mentioned system-level energy efficiency studies to the case of broadband links based on MIMO-OFDM. Therefore, we investigate the performance versus energy efficiency tradeoff of two typical multiantenna techniques—space-time block code (STBC) [3] and space-division multiplexing (SDM)

[4]—and compare it to the single-antenna case. Both are implemented on top of a legacy OFDM transmission chain as used in IEEE 802.11a/g/n and proceed to spatial processing at the receiver only. The IEEE 802.11 MAC has been adapted to accommodate those transmission modes. For the sake of clarity, without hampering the generality of the proposed approach, we limit the study to  $2 \times 2$  antennas systems.

Second, we propose *smartMIMO*, a coarsely adaptive MIMO-OFDM scheme that, on a packet-per-packet basis, switches between STBC, SDM, and SISO depending on the channel conditions to simultaneously secure the throughput and/or robustness improvement provided by the multiantenna transmission and guarantees an energy-efficiency improved compared with the current standards. Contrarily in other adaptive scheme [12–16], using SISO still reveal effective in many channel condition because of the saving in static power consumption.

The remainder of the paper is structured as follows. In Section 2, we present some related work. The MIMO-OFDM physical (PHY) and medium access control (MAC) layers are described in Section 3. The unified performance and energy models used to investigate the average throughput versus energy-efficiency tradeoff are presented in Section 4. The impact of SDM and STBC on the net throughput versus energy-efficiency tradeoff is discussed in Section 5. Finally, in Section 6, we present the *smartMIMO* scheme and evaluate its benefit on the aforementioned tradeoff.

## 2. RELATED WORK

The question whether multiantenna techniques increase or decrease the energy efficiency has only very recently been addressed. Based on comprehensive first order energy and performance models targeted to narrow-band single carrier transceivers (as usually considered in wireless microsensor), Shuguang et al. have evaluated, taking both static and dynamic power consumption into account, the impact on energy efficiency of single-carrier space-time block coding (STBC) versus traditional single antenna (SISO) transmission [9]. Interestingly, it is shown that in short-/middle-range applications such as sensor networks—and by extension, wireless local area networks (WLANs)—nonadaptive STBC actually degrades the system energy efficiency at same data rate. However, when combined with adaptive modulation in so-called adaptive multiantenna transmission, energy-efficiency can be improved. Liu and Li have extended those results by showing that energy-efficiency can further be improved by adaptively combining multiplexing and diversity techniques [10, 11]. Adaptive schemes are hence mandatory to achieve both high-throughput and energy-efficient transmissions.

In the context of broadband wireless communication, many adaptive multiantenna schemes have also been proposed and are often combined with orthogonal frequency division multiplexing (OFDM). Adaptation is most often carried out to minimize the bit-error (BER) probability or maximize the throughput. In [12], for instance, a scheme is proposed to switch between diversity and multiplexing codes based on limited channel state information (CSI) feedback.

In [13], a pragmatic *coarse grain* adaptation scheme is evaluated. Modulation, forward error correction (FEC) coding rate and MIMO encoding are adapted according to CSI estimator—specifically, the average signal-to-noise ratio (SNR) and packet error rate (PER)—to maximize the effective throughput. More recently, *fine grain* adaptive schemes have been proposed [14, 15]. The modulation and multi-antenna encoding are here adapted on a carrier-per-carrier basis. The main challenge with such schemes is however to provide the required CSI to the transmitter with minimal overhead. This aspect is tackled, for instance in [16].

The approaches mentioned above have been proven to be effective to improve net throughput and/or bit-error rate (BER). Some are good candidate to be implemented in commercial chipset. However, in none of those contributions, the electronics power consumption is considered in the optimization. Moreover, most adaptive policies are designed to maximize gross data-rate and/or minimize (uncoded) bit-error rate without taking into account the coupling between physical layer data rate and bit-error rate incurred in medium access control (MAC) layer [17].

In this paper, adaptive MIMO-OFDM schemes are looked at with as objective to jointly optimize the average link throughput (on top of the medium access control layer) and the average transceiver energy efficiency. The total transceiver power consumption is considered, including the terms that vary with the transmit power and the fixed term due the radio electronics.

To enable low-complexity policy-based adaptation and to limit the required CSI feedback, coarsely adaptive schemes, as defined in [13], are considered. For this, pragmatic empirical performance, energy, and channel state information models are developed based on observation and measurements collected on the reconfigurable MIMO-OFDM setup previously described in [18].

### 3. MIMO PHYSICAL AND MAC LAYERS

#### 3.1. MIMO-OFDM physical layer

The multiantenna schemes considered here are orthogonal space-time block coding (STBC) [2, 3] and space-division multiplexing with linear spatial processing at the receiver (SDM-RX) [4]. Both are combined with OFDM so that multiantenna encoding and/or receive processing is performed on a per-carrier basis. The  $N$  OFDM carriers are QAM-modulated with a constellation size set by the link adaptation policy presented in [17]. The same constellation is considered for the different carriers of a given symbol, therefore we refer to “coarse grain” adaptation in opposition to fine grain adaptation where the subcarriers can receive different constellation.

Figure 2 illustrates the general setup for MIMO-OFDM on which either SDM or STBC can be implemented.

For SDM processing, a configuration with  $U$  transmit antenna and  $A$  receive antenna is considered. The multiantenna preprocessing reduces to demultiplexing the input stream in sub-streams that are transmitted in parallel. Vertical encoding is considered: the original bit stream is FEC encoded,

interleaved, and demultiplexed between the OFDM modulators. The MIMO processors at the receiver side take care of the spatial interference mitigation on a per-subcarrier basis. We consider a minimum mean-square-error-(MMSE-) based detection algorithm. Although the MMSE algorithm is outperformed by nonlinear receiving algorithm such as successive interference cancellation [4], its implementation ease keeps it attractive in low-cost, high-throughput solution such as wireless local area networks.

In STBC mode, space-time block codes from orthogonal designs [2, 3] are considered. Such scheme reduces to an equivalent diagonal system that can be interpreted as a SISO model where the channel is the quadratic average of the MIMO sub-channels [3].

Channel encoding and OFDM modulation are done according to the IEEE 802.11a standard specifications, transmission occurs in the 5 GHz ISM band [19].

As mentioned previously, from the transceiver energy-efficiency perspective, it may still be interesting to operate transmission in single-antenna mode. In that case, a single finger of the transmitter and receiver are activated and the MIMO encoder and receive processor are bypassed.

#### 3.2. Medium access control layer

The multiantenna medium access control (MAC) protocol we consider is a direct extension of the IEEE 802.11 distributed coordination function (DCF) standard [19]. A carrier sense multiple access/collision avoidance (CSMA/CA) medium access procedure performs automatic medium access sharing. Collision avoidance is implemented by mean of the exchange of request-to-send (RTS) and clear-to-send (CTS) frames. The data frames are acknowledged (ACK). The IEEE 802.11 MAC can easily be tuned for adaptive multiantenna systems. We assume that the basic behavior of each terminal is single-antenna transmission. Consequently, single-antenna exchange establishes the multiantenna features prior to the MIMO exchange. This is made possible via the RTS/CTS mechanism and the data header. A signaling relative to the multiple-antenna mode is added to the physical layer convergence protocol (PLCP) header.

Further, the transactions required for channel estimation need to be adapted. In the considered  $2 \times 2$  configuration, not only one but four-channel path must be identified. Therefore, the preamble structure is adapted as sketched in Figure 3. The transmitter sends preambles consecutively on antennas 1 and 2. The receiver can then easily identify all channel paths. The complete protocol transactions to transmit a packet of data in the SDM and STBC modes are detailed in Figures 4 and 5, respectively. For SISO transmission, one relies on the standard 802.11 CSMA/CA transaction and on the standard preambles.

### 4. UNIFIED PERFORMANCE AND ENERGY MODEL

The physical (PHY) and medium access control (MAC) layers being known, one wants to compute the net throughput (on top of the MAC) and the energy per bit as functions of the transmission parameters, including the type of

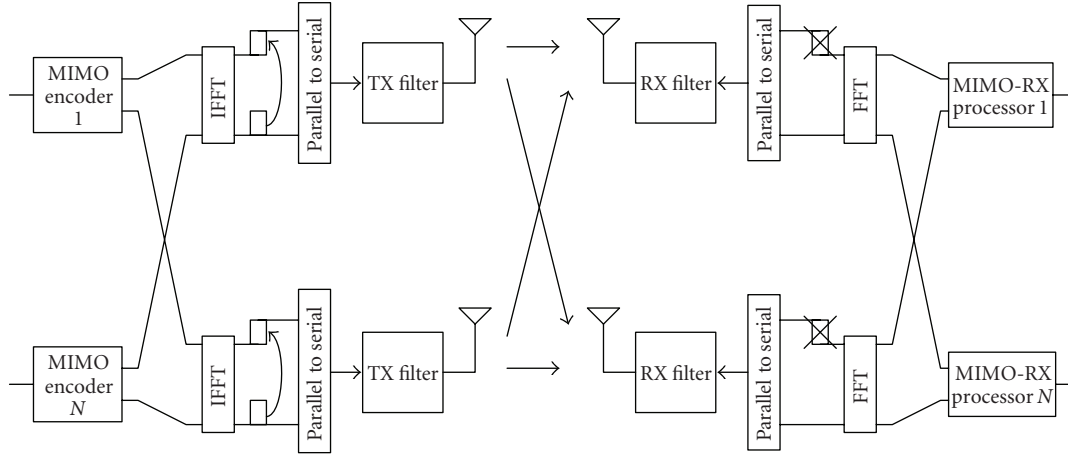


FIGURE 2: Reconfigurable multiantenna transceiver setup supporting SDM, STBC, and SISO transmissions.

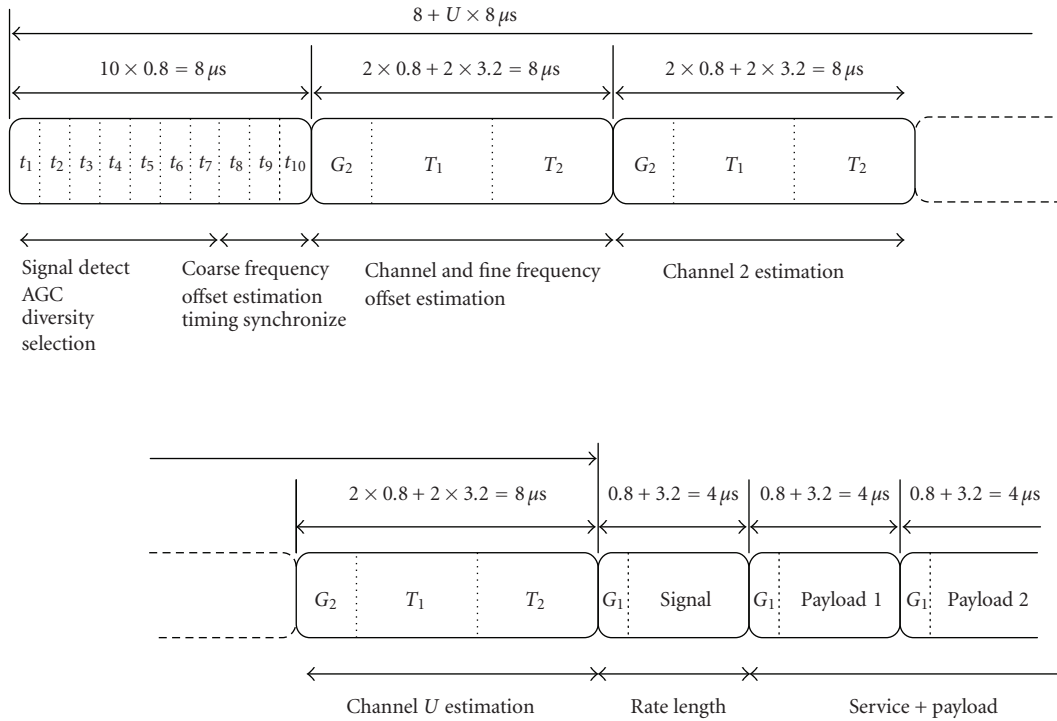


FIGURE 3: Channel estimations from the preamble for a  $2 \times 2$  system.

multiantenna processing, and the channel state. To enable simple policy-based adaptation scheme and limit the required CSI feedback, a coarse channel state model is needed to capture the CSI in a synthetic way. The proposed model should cover the system performance and energy consumption of the different multiantenna techniques under consideration.

An important aspect is to identify tractable channel state parameters that dominate the instantaneous packet error probability. The average packet errors rate (PER) as tradi-

tionally evaluated misses that instantaneous dimension. In narrow-band links affected by Rayleigh fading, the signal-to-noise ratio (SNR) suffices to track the channel state. In MIMO-OFDM, however, the impact of the channel is more complex. With spatial multiplexing, for instance, the error probability for a given modulation and SNR still depends on the rank of the channel. Moreover, not all the subcarriers experience the same MIMO channel. Finally, a given channel instance can be good for a specific MIMO mode while being bad for another one.

- (1) TX sends RTS in SISO. the PLCP header contains:
  - (i) 2 bits specifying the MIMO exchange type (here channel state extraction at RX)
  - (ii) 2 bits for the number of TX antennas that will be activated for the next MIMO exchange ( $n_{TX}$ ) and that have to be considered in the channel extraction
  - (iii) 2 bits for the minimum numbers of RX antennas to activate for next reception.
- (2) RX sends CTS.
- (3) TX send DATA preambles in time division: 10 short training sequences for coarse synchronization ( $t_1 \cdots t_{10} - 8 \mu s$ ) and  $2 \times n_{TX}$  long training sequences ( $G_2 T_1 T_2 - 8 \mu s$ , called C-C sequence). Each TX antenna transmits after each other its C-C sequence. RX activates its antennas and extracts information about each channel that each antenna sees. PLCP header is sent from the last TX antenna and conveys 2 bits for the mode (here SDM-RX) and 2 bits for the number of streams. finally, TX sends the DATA in MIMO.
- (4) RX sends ACK.

FIGURE 4: Considered SDM protocol extension.

- (1) TX sends RTS in SISO. the PLCP header contains:
  - (i) 2 bits specifying the MIMO exchange type (here channel state extraction at RX)
  - (ii) 2 bits for the number of TX antennas that will be activated for the next MIMO exchange ( $n_{TX}$ ) and that have to be considered in the channel extraction
  - (iii) 2 bits for the minimum numbers of RX antennas to activate for next reception.
- (2) RX sends CTS.
- (3) TX send DATA preambles in TDMA: 10 short training sequences for coarse synchronization ( $t_1 \cdots t_{10} - 8 \mu s$ ) and  $2 \times n_{TX}$  long training sequences ( $G_2 T_1 T_2 - 8 \mu s$ , called C-C sequence). Each TX antenna transmits after each other its C-C sequence. RX activates its antennas and extracts information about each channel that each antenna sees. PLCP header is sent from the last TX antenna and conveys 2 bits for the mode (here STBC) and 4 bits for the code used. Finally, TX sends the DATA in MI-SO/MO depending on the number of recieved antenna ( $n_{RX}$ ).
- (4) RX sends ACK.

FIGURE 5: Considered STBC protocol extension.

Possible coarse channel state information (CSI) indicators for MIMO-OFDM are discussed in [13]. An empirical approach based on multiple statistics of the postprocessing SNR (the SNR after MIMO processing) and running-average PER monitoring is proposed. Yet, it is difficult to define such SNR-based indicators consistently across different MIMO schemes. Moreover, relying on PER information

results in a tradeoff between accuracy and feedback latency, both with potential impact on stability.

As already proposed in [20], based on the key observation that energy efficiency and net throughput are actually weak functions of the packet error probability [21], we prefer to use the outage probability—that is, the probability that the channel instantaneous capacity is lower than the link spectrum efficiency—as indicator of the packet error probability. The instantaneous capacity depends on the average signal-to-noise ratio (SNR), the normalized instantaneous channel response  $\mathbf{H}$ , and the multiantenna encoding. The instantaneous capacity can be easily derived for the different multi-antenna encoding. Practically, it is convenient to derive the capacity-over-bandwidth ratio that can be compared to the transmission spectrum efficiency  $\eta$  instead of absolute rate.

In the remainder of this session, we first derive the instantaneous capacity expressions for the different transmission mode considered (Section 4.1). Then, we derive the condition for quasi-error-free packet transmission (Section 4.2). Based on that, we compute the expressions of the net throughput and the energy per bit (Sections 4.3 and 4.4). Finally, we discuss the derivation of the coarse channel model required to develop policy-based radio link control strategies (Section 4.5).

#### 4.1. Instantaneous capacity

Let  $\mathbf{H} = (h_{ua}^n)$  be a normalized MIMO-OFDM channel realization. The coefficient  $h_{11}^n$  corresponds to the (flat) channel response between the single active transmit antenna and the single active receive antenna for the subcarrier  $n$  (including transmit and receive filters). The *instantaneous capacity* of the single-antenna channel is given by (1), where  $W$  is the signal bandwidth and  $N$  is the number of subcarriers. SNR is the average link signal-to-noise ratio. If SNR is high compared to 1, the capacity relative to the bandwidth can be decomposed in a term proportional to SNR and independent of  $\mathbf{H}$  and a second term function of  $\mathbf{H}$  only:

$$C = W \cdot \frac{1}{N} \sum_{n=1}^N \log_2(1 + h_{11}^{n2} \text{SNR}), \quad (1)$$

$$\frac{C}{W} \cong \frac{\text{SNR}|_{\text{dB}}}{10 \log_{10} 2} + \frac{1}{N} \sum_{n=1}^N \log_2(h_{11}^{n2}). \quad (2)$$

In the STBC case, as mentioned in Section 3, the MIMO channel can be reduced to equivalent SISO channel corresponding to the quadratic average of the subchannels between each pairs of transmit and receive antennas [3]. The *instantaneous capacity* can then be computed just as for SISO:

$$\frac{C}{W} \cong \frac{\text{SNR}|_{\text{dB}}}{10 \log_{10} 2} + \frac{1}{N} \sum_{n=1}^N \log_2 \left( \frac{1}{UA} \sum_{u=1}^U \sum_{a=1}^A h_{ua}^{n2} \right). \quad (3)$$

In the SDM case finally, the compound channel results from the concatenation of the transmission channel with the interference cancellation filter. The instantaneous capacity can be computed based on the *postprocessing SNR's* ( $\gamma$ )—that is, for each stream, the signal-to-noise-and-interference ratio at



the output of the interference cancellation filter. Let  $\mathbf{H}^n$  and  $\mathbf{F}^n$ , respectively, denote the MIMO channel realization for the subcarrier  $n$ , and the corresponding MMSE filter (4):

$$\mathbf{F}^n = \mathbf{H}^{nH} \cdot (\mathbf{H}^n \mathbf{H}^{nH} + \sigma^2 \mathbf{I}_{AxA})^{-1}. \quad (4)$$

In the considered  $2 \times 2$  case, let us assume an equal transmit power at both transmit antennas  $p_1 = p_2 = p/2$  and let us denote with  $\mathbf{f}_1^n$ ,  $\mathbf{f}_2^n$ ,  $\mathbf{h}_1^n$ ,  $\mathbf{h}_2^n$ , respectively, the first row, second row, first column, second column of the matrices  $\mathbf{H}^n$  and  $\mathbf{F}^n$ . The substream postprocessing SNRs  $\gamma_1$  and  $\gamma_2$  can then be computed as

$$\gamma_1^n = \frac{|\mathbf{f}_1^n \mathbf{h}_1^n|^2 \times P_1}{|\mathbf{f}_1^n \mathbf{h}_2^n|^2 \times P_2 + |\mathbf{f}_1^n|^2 \times \sigma^2} = \frac{|\mathbf{f}_1^n \mathbf{h}_1^n|^2}{|\mathbf{f}_1^n \mathbf{h}_2^n|^2 + |\mathbf{f}_1^n|^2 \times 2/\text{SNR}},$$

$$\gamma_2^n = \frac{|\mathbf{f}_2^n \mathbf{h}_2^n|^2 \times P_2}{|\mathbf{f}_2^n \mathbf{h}_1^n|^2 \times P_1 + |\mathbf{f}_2^n|^2 \times \sigma^2} = \frac{|\mathbf{f}_2^n \mathbf{h}_2^n|^2}{|\mathbf{f}_2^n \mathbf{h}_1^n|^2 + |\mathbf{f}_2^n|^2 \times 2/\text{SNR}}. \quad (5)$$

SNR is again the average link signal-to-noise ratio. The instantaneous *capacity* can then be computed in analogy with (2) and (3) as follows:

$$\frac{C}{W} = \frac{1}{N} \sum_{n=1}^N [\log_2(1 + \gamma_1^n) + \log_2(1 + \gamma_2^n)]. \quad (6)$$

This development can easily be extended to more than  $2 \times 2$  antenna setups.

#### 4.2. Condition for quasi-error-free packet transmission on a given channel

Because the link throughput and energy efficiency (our objective functions) are weak functions of the packet error probability [21], one does not need to estimate the latter accurately in order to define adaptation policies that optimize the formers. It is sufficient to derive a condition under which the packet error rate is sufficiently low in order not to significantly affect the aforementioned objective functions. It is easy to verify that the accuracy obtained on the throughput on top of the MAC and on the energy efficiency is of the same order of magnitude that the packet error rate.

Based on Monte Carlo simulations, we have verified that, for the purpose of computing the average throughput on top of the MAC and the transceiver energy consumption per bit, the packet error event probability can be approximated by the outage without significant prejudice to the accuracy (Figure 6). We hence assume that, the channel being known,  $P_e$ , equals 1 if the spectrum efficiency  $\eta$  exceeds  $C/W$ . To account for the nonoptimality of the coding chain, we apply an empirical margin  $\delta = 0.5$  bit/s/Hz, calibrated from simulation:

$$P_e = \begin{cases} 1 & \text{if } \frac{C}{W} < \eta + \delta, \\ \cong 0 & \text{otherwise.} \end{cases} \quad (7)$$

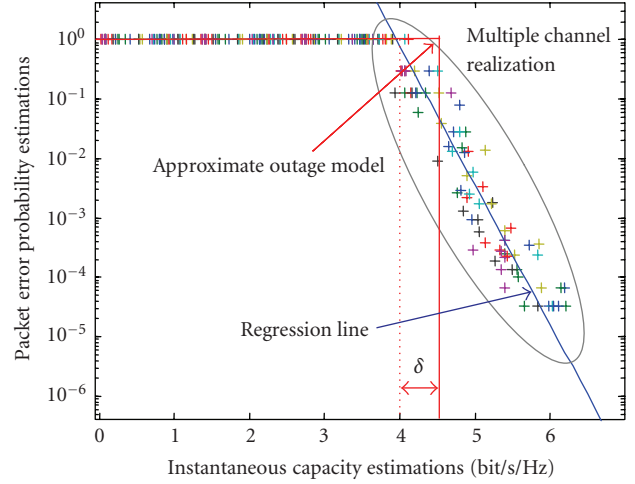


FIGURE 6: Packet error probability and instantaneous capacity observation on a link with spectrum efficiency 4 for a large set of channel realizations. One can observe the strong correlation and the steep descend of the regression line beyond the point where the instantaneous capacity breaks the spectrum efficiency line. The net throughput and energy per bit are weak function of the packet error probability; these observations motivate considering an outage model to derive policy-based adaptive schemes.

#### 4.3. Net throughput

Assuming that the channel capacity criteria is met and, hence, the PER is close to zero, knowing the physical layer throughput ( $R_{\text{phy}}$ ) and the details of the protocols, the *net throughput* ( $R_{\text{net}}$ ) can be computed as follows:

$$R_{\text{net}} \cong \frac{L_d}{T_{\text{DIFS}} + 3 \cdot T_{\text{SIFS}} + T_{\text{CW}} + ((L_d + L_h)/R_{\text{phy}}^d) + 4 \cdot T_{\text{plcp}} + L_{\text{ctrl}}/R_{\text{phy}}^b}. \quad (8)$$

To better understand that expression, refer to Figure 7 and notice that the denominator corresponds to the total time required for the transmission of one packet of data size  $L_d$  with a  $L_h$ -bit header according to the 802.11 DCF protocol [19].  $T_{\text{SIFS}}$  is the so-called short interframe time.  $R_{\text{phy}}^d$  is the physical layer data rate.  $L_{\text{ctrl}}$  corresponds to the aggregate length of all control frames (RTS, CTS, and ACK) transmitted at the basic rate ( $R_{\text{phy}}^b$ ) and  $T_{\text{plcp}}$  is the transmission time of the PLCP header.  $T_{\text{DIFS}}$  is the minimum carrier sense duration and  $T_{\text{CW}}$  holds for the average contention time due to the CSMA procedure. The physical layer data rate  $R_{\text{phy}}^d$  can be expressed as a function of modulation order ( $N_{\text{mod}}$ ) and the code rate ( $R_c$ ), considering the number of data carrier per OFDM symbol ( $N$ ) and the symbol rate ( $R_s$ ), in addition to the number of streams  $U$  (9). In our study, one has  $U = 1$  for SISO and  $U = 2$  for both SDM and STBC. In the MIMO case ( $U > 1$ ), one of the four  $T_{\text{PLCP}}$ 's in (8) must be replaced by  $T_{\text{PLCP\_MIMO}}$  given in (10) with  $T_{\text{CC\_Seq}}$  being equal  $8 \mu\text{s}$ :

$$R_{\text{phy}}^d = U \cdot N \cdot N_{\text{mod}} \cdot R_c \cdot R_s, \quad (9)$$

$$T_{\text{PLCP\_MIMO}} = T_{\text{PLCP\_SISO}} + (U - 1) \times T_{\text{CC\_Seq}}. \quad (10)$$

#### 4.4. Energy per bit

To compute the energy efficiency, the system power consumption needed to sustain the required average SNR must be assessed. The latter consists of a fixed term due to the electronics, and a variable term, function of the power consumption

$$P_{\text{system}} = P_{\text{elec}} + \frac{P_{\text{Tx}}}{\varepsilon}, \quad (11)$$

where  $\varepsilon$  denotes the efficiency of the transmitter power amplifier (PA), that is, the ratio of the output power ( $P_{\text{Tx}}$ ) by the power consumption ( $P_{\text{PA}}$ ). In practical OFDM transmitters, class A amplifiers are typically used. The power consumption of the latter component only depends on its maximum output power ( $P_{\text{max}}$ ) (12). Next, the transmitter signal-to-distortion ratio ( $S/D_{\text{Tx}}$ ) can be derived as a function of the sole backoff (OBO) of the actual PA output power ( $P_{\text{Tx}}$ ) to  $P_{\text{max}}$  (13)-(14). The latter relation is design dependent and usually not analytical. In this study, we consider an empirical curve-fitted model calibrated on the energy-scalable transmission chain design presented in [8], which has as key feature to enable both variable output power ( $P_{\text{Tx}}$ ) and variable linearity ( $S/D_{\text{Tx}}$ ) with a monotonic impact on the power consumption;

$$P_{\text{PA}} = \frac{P_{\text{max}}}{2}, \quad (12)$$

$$\text{OBO} = \frac{P_{\text{max}}}{P_{\text{Tx}}}, \quad (13)$$

$$(S/D)_{\text{Tx}} = f(\text{OBO}). \quad (14)$$

The path-loss being known, SNR can then be computed as a function of OBO and  $P_{\text{Tx}}$  (15).  $P_{\text{N}}$  is the thermal noise level depending of the temperature ( $T$ ), the receiver bandwidth ( $W$ ), and noise factor ( $N_f$ ),  $k$  is the Boltzmann constant:

$$\frac{1}{\text{SNR}} = \frac{1}{(S/D)_{\text{Tx}}} + \frac{P_{\text{N}} \times P_{\text{L}}}{P_{\text{Tx}}}, \quad (15)$$

$$P_{\text{N}} = k \cdot T \cdot W \cdot N_f. \quad (16)$$

The PA power can be expressed as a function of those two parameters (17):

$$P_{\text{PA}} = 2 \times (P_{\text{Tx}} \times \text{OBO}). \quad (17)$$

The achievable  $P_{\text{PA}}$  versus SNR tradeoff obtained with the design as presented in [8] is illustrated for different average link path-loss values in Figure 8. Notice that in case the output power has to stay constant, the proposed reconfigurable architecture still has the possibility to adapt to the linearity requirements. This has less but still significant impact on the power consumption.

#### 4.5. Coarse channel model

At this point in the development, we have relations to compute the link throughput and the transceiver energy consumption per bit for given multiantenna encoding, modu-

lation and code rate, provided that the link SNR is sufficient to satisfy the quasi error free transmission condition.

The latter condition depends also on the actual channel response  $\mathbf{H}$  (equations (2), (3), (5), (6), and (7)). Extensive work has already been done to model broadband channel at that level of abstraction (physical level). In the case of MIMO-OFDM WLAN as considered here, a reference channel model is standardized by the IEEE [22]. However, to be able to derive simple policy-based adaptation schemes that take that channel state information into account, one has to derive a model that captures this information in a more compact way. A valid approach is to operate an empirical classification of the channel merit. This can easily be done based on the instantaneous capacity indicators.

As an example, let us consider the second term of the instantaneous SISO capacity. According to [22], the values of the carrier fading  $h_{ua}^n$  are Rayleigh distributed. However, due to the averaging across the carriers, which are only weakly correlated, the distribution of the second term of the instantaneous capacity is almost normal distributed (see Figure 9). Since the first term of the capacity indicator is independent of  $\mathbf{H}$  and therefore not stochastic, the capacity indicator can then also be approximated as normal-distributed. One can verify that the same observation holds also for the STBC and SDM instantaneous capacity indicators (see Figure 9).

Let us, respectively, denote the average and variance of the instantaneous capacity for a given mode as  $\mu_{\text{mode}}$  and  $\sigma_{\text{mode}}^2$ . These quantities depend only on SNR. Their evolution in a function of SNR is plotted in Figure 10 for the different multiantenna encoding. It can be observed that for a given mode and a sufficiently large SNR,  $\mu_{\text{mode}}$  grows linearly with SNR in dB while  $\sigma_{\text{mode}}^2$  stays sensibly constant. Therefore, a linear regression can be operated. The parameters of the extracted linear model are summarized in Table 1.

Based on the normal distribution of the instantaneous capacity and the linear models for the parameters of that distribution, a channel merit scale can be defined. A given channel instance receives a merit index for a given multi-antenna mode and a given SNR depending on how its actual instantaneous capacity compared to the capacity distribution for that mode and that SNR. The empiric scale we consider goes from 1 (worst) to 5 (best) with the class boundaries as defined in Table 2 (3 first columns).

For each class index (channel merit), a worst-case error-free transmission condition is defined, comparing the signaling spectrum efficiency ( $\eta$ ) to the upper bound of the instantaneous capacity class for this channel merit (Table 2, fourth column).

#### 4.6. Usage of the model

One can now compute, for a given channel merit as defined above, what will be the link throughput and the transceiver energy consumption per bit for a given multiantenna mode, a given modulation and a given code rate. The computation occurs as follows.

*Step 1.* Knowing the modulation and code rate, hence the signaling spectrum efficiency, the minimum link SNR to

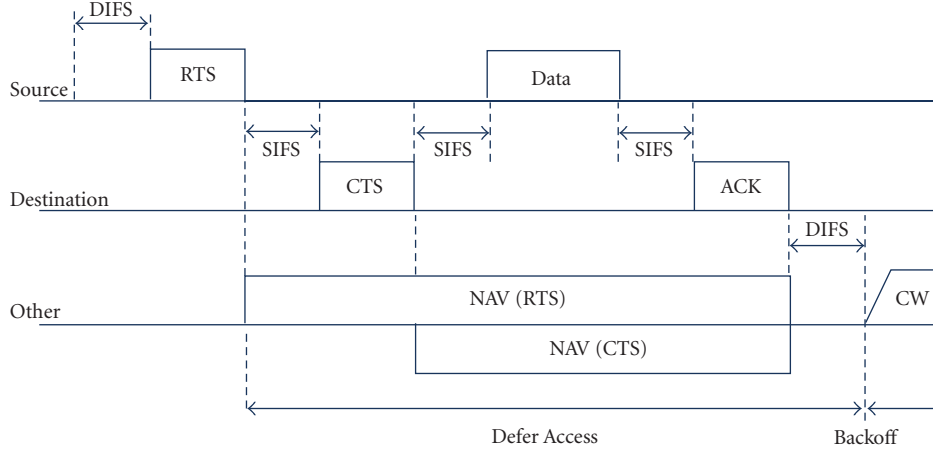


FIGURE 7: Packet transmission transaction according to the IEEE 802.11 protocol modified to support multiantenna operation.

TABLE 1: Instantaneous capacity indicator average and standard deviation as a function of the average SNR.

	$\mu = A \times \text{SNR} + B$		$\sigma$
	A	B	
SISO	0.33	-0.84	1.41
SDM	0.6	-2.54	2.41
STBC	0.33	-0.24	0.73

satisfy the worst-case quasi-error-free transmission condition (for the given multi-antenna mode and channel merit) is computed using the appropriate inequality from Table 2, fourth column, and the linear model exposed in Table 1.

*Step 2.* Knowing the multi-antenna mode, the modulation and the code rate, assuming quasi-packet-error-free transmission, the link throughput is computed according to (8). The condition is calibrated for a packet error rate of <1%, yielding an accuracy of 1% of the estimated throughput and energy efficiency.

*Step 3.* Based on the power model exposed in Section 4.4, assuming a given average path loss, the transmitter parameters (output power, backoff) to achieve the link SNR computed in Step 1, and subsequently the transmitter power consumption, are computed.

*Step 4.* From the transmitter power and the net throughput, the energy per bit can be computed.

## 5. IMPACT OF MIMO ON THE AVERAGE RATE VERSUS AVERAGE POWER TRADEOFF

The proposed performance and energy models enable computing the net throughput and energy efficiency as functions of the system-level parameters (mode, modulation, code rate, transmit power, and power amplifier backoff). The

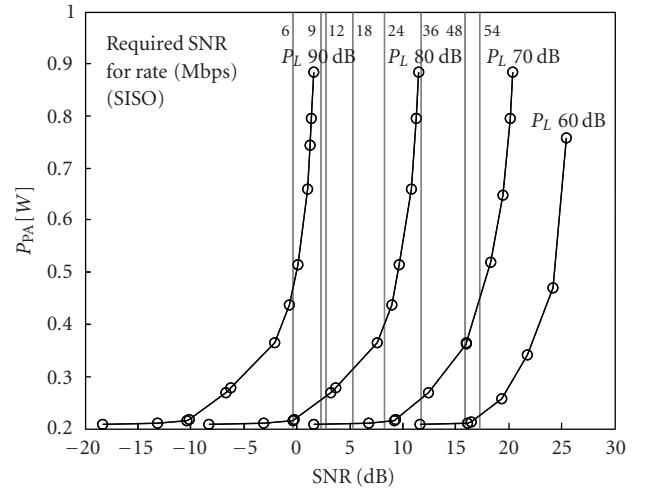


FIGURE 8: Power consumption versus link SNR tradeoff achieved with the energy scalable transmitter for average path-loss,  $P_L = 60$  dB, 70 dB, 80 dB, 90 dB. The tradeoff curves are compared to the SNR level required for 20 MHz SISO-OFDM transmission with PER < 10% at various rates.

considered settings for those parameters are summarized in Table 3. Capitalizing on those models and using the techniques already proposed in [17], one can derive a set of close-to-optimal transmission adaptation policies that optimize the average energy efficiency for a range of average throughput targets and, then, analyze the resulting tradeoff.

In this section, we derive these tradeoffs separately for the STBC and SDM modes and compare with SISO. This is done in two steps.

*Step 1.* For each channel merit, the optimum tradeoff between net throughput and energy per bit (Section 5.1) is derived. This results in a Pareto optimal [23] set of working points (settings of the system-level parameters) for each possible channel merit.



TABLE 2: Definition of the channel merit.

Channel merit	Channel instance instantaneous capacity indicator		Maximum spectrum efficiency for quasi error free transmission
	Min	Max	
1	$-\infty$	$\mu_{\text{mode}} - 2 \times \sigma_{\text{mode}}$	—
2	$\mu_{\text{mode}} - 2 \times \sigma_{\text{mode}}$	$\mu_{\text{mode}} - \sigma_{\text{mode}}$	$\eta < \mu_{\text{mode}}(\text{SNR}) - 2 \times \sigma_{\text{mode}}(\text{SNR})$
3	$\mu_{\text{mode}} - \sigma_{\text{mode}}$	$\mu_{\text{mode}} + \sigma_{\text{mode}}$	$\eta < \mu_{\text{mode}}(\text{SNR}) - \sigma_{\text{mode}}(\text{SNR})$
4	$\mu_{\text{mode}} + \sigma_{\text{mode}}$	$\mu_{\text{mode}} + 2 \times \sigma_{\text{mode}}$	$\eta < \mu_{\text{mode}}(\text{SNR}) + \sigma_{\text{mode}}(\text{SNR})$
5	$\mu_{\text{mode}} + 2 \times \sigma_{\text{mode}}$	$+\infty$	$\eta < \mu_{\text{mode}}(\text{SNR}) + 2 \times \sigma_{\text{mode}}(\text{SNR})$

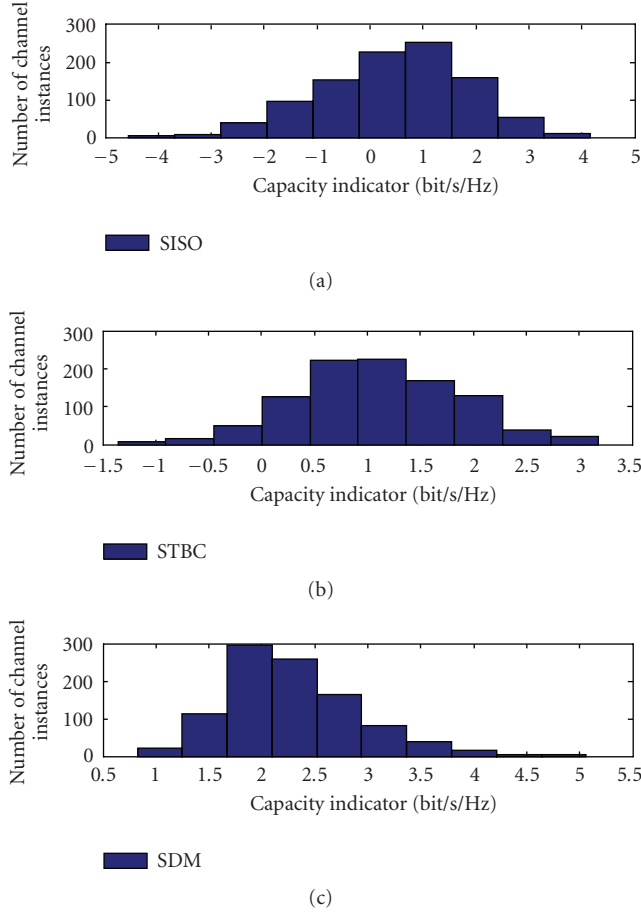


FIGURE 9: Distribution of the instantaneous capacity observation for the different modes (SISO, STBC, SDM) over a large set of channel instances generated with the physical channel model.

Step 2. For a given average throughput target, a policy is derived to select which working points from the Pareto optimal set has to be used for each channel merit value in order to minimize the average energy per bit (Section 5.2).

The resulting average throughput versus energy-per-bit tradeoffs is finally analyzed in Section 5.3. It should be noticed that this approach assume that the channel merit is known at the transmitter (limited CSI at transmit). That information can be acquired during the reception of the CTS

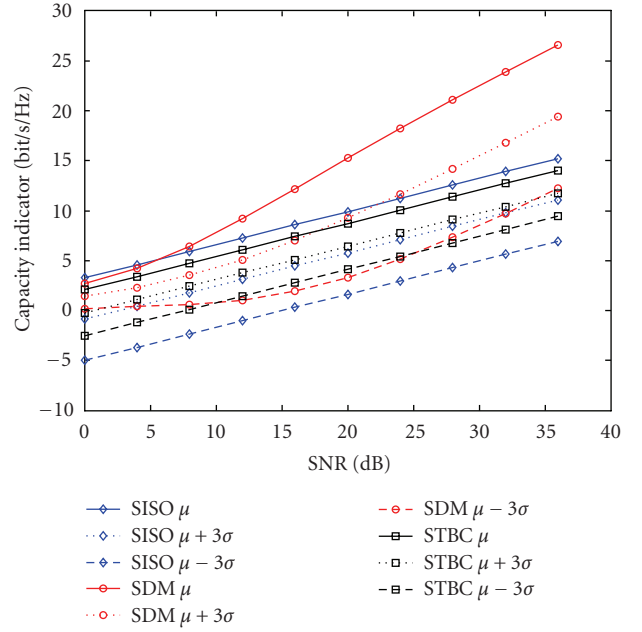


FIGURE 10: Capacity indicator mean and standard deviation as a function of SNR for the various modes.

TABLE 3: System-level parameters considered.

MIMO mode	SISO, SDM2 × 2, STBC2 × 2
$N_{\text{mod}}$	BPSK, QPSK, 16QAM, 64QAM
$R_c$	1/2, 2/3, 3/4
$P_{\text{Tx}}$ [dBm]	0, 5, 10, 15, 20, 23
OBO [dB]	6, 8, 10, 12, 14

frame or piggy-backed in the CTS, assuming that the channel is stable during RTS/CTS/packet transaction. The assumption is valid in nomadic scenario as considered in case of WLAN (typical coherence time of 300 milliseconds).

### 5.1. Net throughput versus energy-per-bit

To derive the optimal net throughput versus energy-per-bit tradeoff for a given mode in a given channel merit, a multiobjective optimization problem has to be solved: from

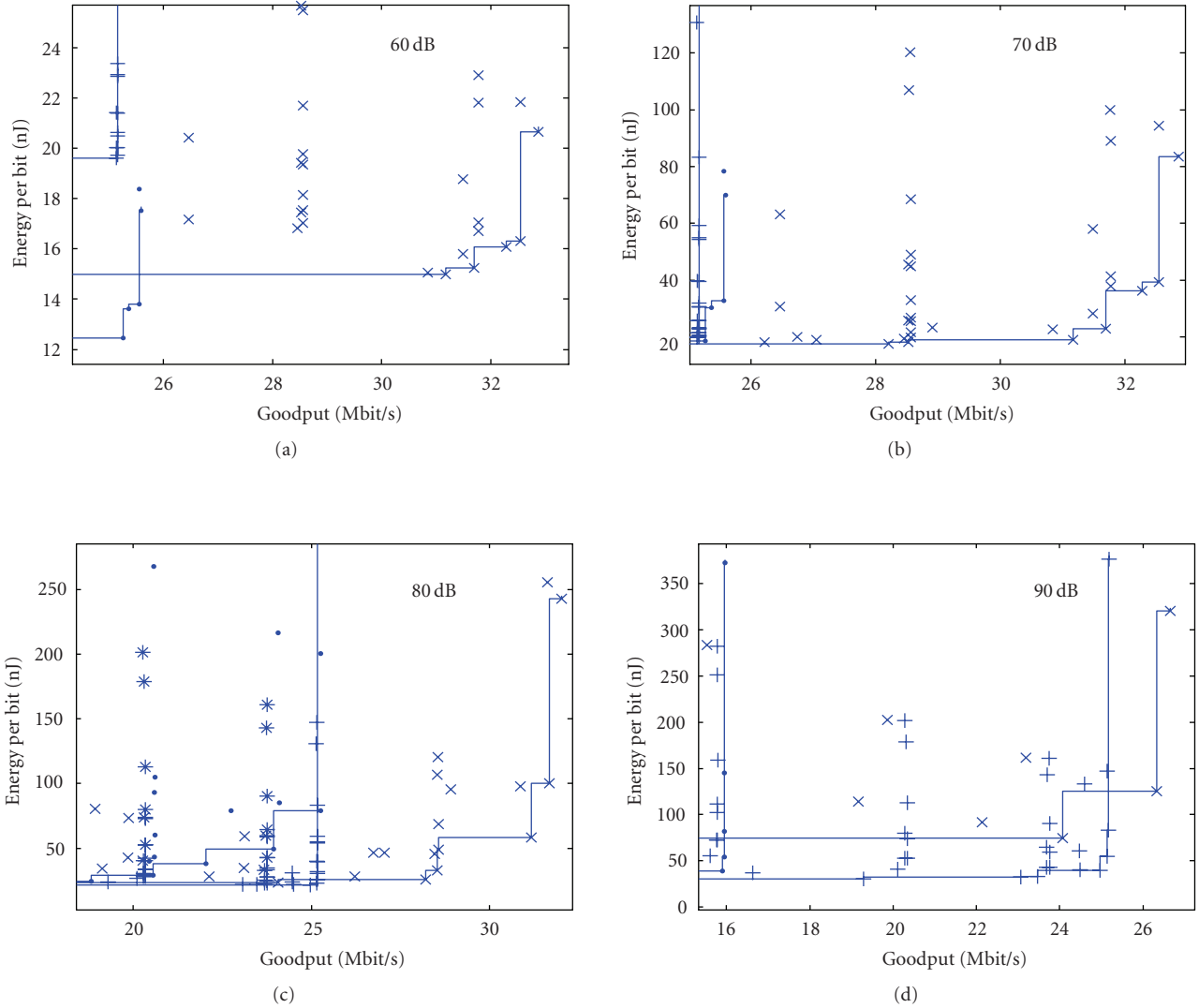


FIGURE 11: Net throughput versus energy-per-bit tradeoff for channel merit 3 and various path-losses. The ( $\cdot$ ) corresponds to the SISO working points, the (+) corresponds to the STBC, and the ( $\times$ ) corresponds to the SDMs. In each case, the Pareto optimal set is interpolated with a step curve.

all system-level parameter combinations, the ones bounding the tradeoff have to be derived. The limited range of the functional parameters still allows us to proceed efficiently to this search with simple heuristics [17]. This optimization can be proceeded to at design time, which limits to a great extent the complexity of the adaptation scheme.

The resulting tradeoff points are plotted in Figure 11 for different path losses and an average channel merit (which is 3). For each mode, we only keep the nondominated tradeoff points, leading to Pareto optimal sets, which are interpolated by step curves. We generally observe that SDM enables reaching higher throughput but that SISO stays more energy efficient for lower rates. STBC becomes attractive in case of large path losses. Similar tradeoff shapes can be observed for the other channel merit values.

## 5.2. Derivation of the control policies

From the knowledge of the Pareto optimal net throughput versus energy-per-bit tradeoff and the channel merit probabilities, which can be obtained from the Monte Carlo analysis of the physical-level channel model, given an average throughput constraint, we applied the technique presented in [17] to derive the adaptation policy that minimizes the energy per transmitted bit. Such a policy, valid for a given multiantenna mode, a given average path loss, and a given average throughput constraints, maps the possible channel merit to the appropriate setting of the transmission parameters.

Let  $(r_{ij}, e_{ij})$  denote the coordinates of the  $i$ th Pareto point in the set corresponding to channel merit  $j$ . The average

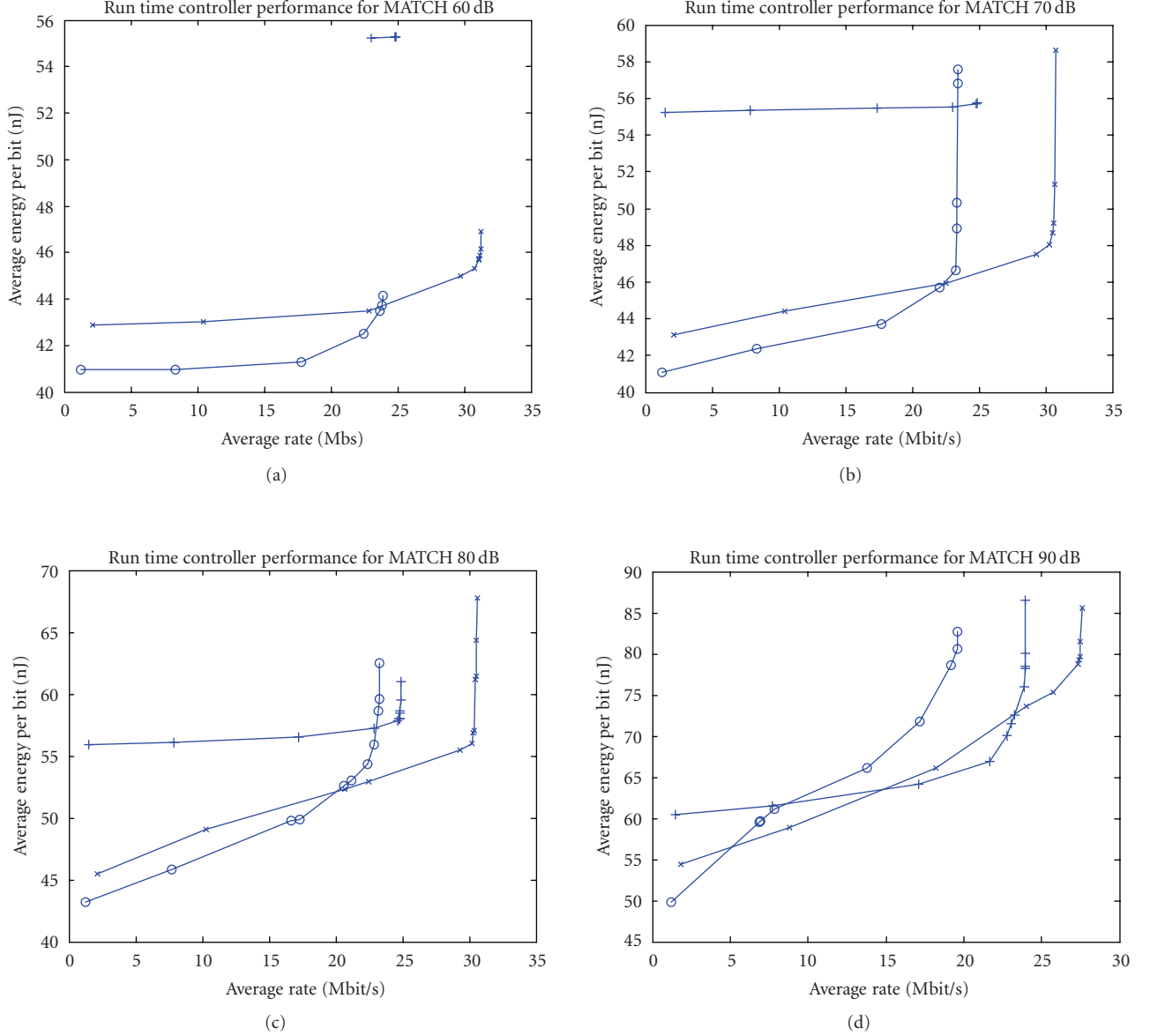


FIGURE 12: Average net throughput versus average energy-per-bit tradeoff for SISO (o), STBC (+), and SDM (x) at various path-loss.

power  $\bar{P}$  and rate  $\bar{R}$  corresponding to a given control policy—that is, the selection of one point on each throughput energy efficiency tradeoff—can then be expressed by (18). In these equations,  $x_{ij}$  is 1 if the corresponding point is selected, 0 otherwise, and  $\psi_j$  is the probability of the channel merit  $j$ . The energy per bit can be computed as  $\bar{P} / \bar{R}$ :

$$\begin{aligned}\bar{P} &= \sum_j \psi_j \sum_i x_{ij} e_{ij} r_{ij} = \sum_i \sum_j x_{ij} \psi_j e_{ij} r_{ij} \hat{=} \sum_i \sum_j x_{ij} p'_{ij}, \\ \bar{R} &= \sum_j \psi_j \sum_i x_{ij} r_{ij} = \sum_i \sum_j x_{ij} \psi_j r_{ij} \hat{=} \sum_i \sum_j x_{ij} r'_{ij}.\end{aligned}\quad (18)$$

We introduce the notation  $p'_{ij}$  and  $r'_{ij}$  corresponding, respectively, to the power and rate when the channel merit is  $j$  and the  $i$ th point is selected on the corresponding curve, both

weighted by the probability to be in that channel state. Only one tradeoff point can be selected for a given channel merit, resulting in the following constraints:

$$\sum_i x_{ij} = 1 \quad \forall j, \quad x_{ij} \in \{0, 1\}.\quad (19)$$

For a given average rate constraint  $R$ , the optimal control policy is the solution of the following problem:

$$\min \sum_i \sum_j x_{ij} p'_{ij} \quad \text{subject to} \quad \sum_i \sum_j x_{ij} r'_{ij} > R.\quad (20)$$

This is the classical multiple choice knapsack problem. We are interested in the family of control policies corresponding to  $R$  ranging from 0 to  $R_{\max}$ ,  $R_{\max}$  being the maximum average rate achievable on the link. We call this family the *control*

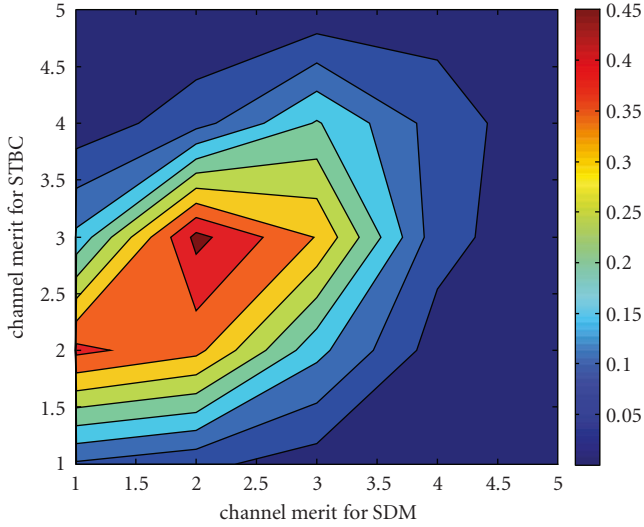


FIGURE 13: Histogram of the channel merit for STBC and SDM.

*strategy*. Let us denote as  $k_j$  the index of the point selected on the  $j$ th Pareto curve. Formally,  $k_j = i \Leftrightarrow x_{ij} = 1$ . A control policy can be represented by the vector  $\mathbf{k} = \{k_j\}$ . The *control strategy*, denoted  $\{\mathbf{k}^{(n)}\}$  corresponds to the set of points  $\{(\bar{R}^{(n)}, \bar{P}^{(n)})\}$  in the average throughput versus average power plane. A good approximation of the optimal control strategy (i.e., that bounds the tradeoff between  $\bar{R}$  and  $\bar{P}$ ) can be derived iteratively with the greedy heuristic explained in [17].

### 5.3. Average throughput versus average energy-per-bit

From the knowledge of the Pareto optimal net throughput versus energy-per-bit tradeoff for each channel merit, next to the channel merit probabilities one can now derive, given an average rate constraint  $\bar{R}$ , the control policy that minimizes the energy per bit. By having the constraint  $\bar{R}$  ranging from 0 to its maximum achievable value  $R_{\max}$ , the average throughput versus average energy-per-bit tradeoff, when applying the proposed policy-based adaptive transmission, can be studied. The tradeoff (for each mode separately) is depicted in Figure 12 for path losses 60, 70, 80, and 90 dB.

The results for SDM and STBC are compared with the tradeoff achieved with a SISO system. One can observe that for low path loss (60–70 dB), SISO reveals, on the average, to be the most energy efficient in almost the whole range it spans. SDM enables, however, a significant increase of the maximum average rate. STBC is irrelevant in this situation. At average path loss (80 dB), a *breakpoint* rate (around 20 Mbps) exists above which both SDM and STBC are more energy efficient than SISO, although SDM is still better than STBC. At high path loss (90 dB), STBC is the most efficient between 20 and 25 Mbps. It is though still beaten by SDM for data rate beyond 25 Mbps and by SISO for smaller data rate.

## 6. SMARTMIMO

In the previous section, we have observed that STBC or SDM enable a significant average rate and/or range extension but hardly improve the energy efficiency. This is especially true when the average data rate is lower than 50% of the ergodic capacity of the MIMO channel.

Based on that observation, in this section, we propose to extend the policy-based adaptive scheme not only to adapt the transmission parameters with a fixed multiantenna encoding, but also to vary the latter encoding on a packet-per-packet basis. Beside, since it has been observed that SISO transmission is still most energy-efficient in certain condition, it is also considered as a possible transmission mode in the adaptive scheme.

Observing the histogram of the channel merits for the reference 802.11n channel model (Figure 13), one can notice that the merit indexes of a given channel for STBC or SDM are weakly correlated. Since the energy efficiency of a given mode is obviously better on a channel with a high merit, an average energy-efficiency improvement can be expected by letting the adaptation policy select one or the other transmission mode depending on the channel state.

### 6.1. Extended adaptation policy

The approach followed in Section 5 can be generalized to handle multiantenna mode adaptation, besides the other transmission parameters. For a given average path-loss and a given average rate target, the adaptation policy will now map a compound channel merit (namely, the triplets of channel merit values for the three possible multiantenna mode) to the system-level parameter settings, extended with the decision on which multiantenna mode to use.

As previous, the adaptation policies are derived in two steps.

*Step 1.* For each possible compound channel merit combination (with our scale,  $5 \times 5 \times 5 = 125$  combinations), the Pareto optimal tradeoff between throughput and energy per bit is derived. This tradeoff can be derived by combining the single-mode Pareto tradeoffs for the corresponding single-mode channel merits. This combined Pareto set corresponds basically to the subset of nondominated points in the union of the Pareto sets to be combined.

*Step 2.* Based on the throughput versus energy-per-bit tradeoff for each compound channel merits and the knowledge of the compound channel merit probabilities, obtained again by Monte Carlo analysis of the physical-level channel model, one can derive the adaptation policy that minimizes the average energy per bit for a given average throughput target. This derivation is identical as in Section 5.

In the remainder, we analyze the average throughput versus energy-per-bit tradeoff achieved by an extended adaptive transmission scheme and compare to the results from Section 5.

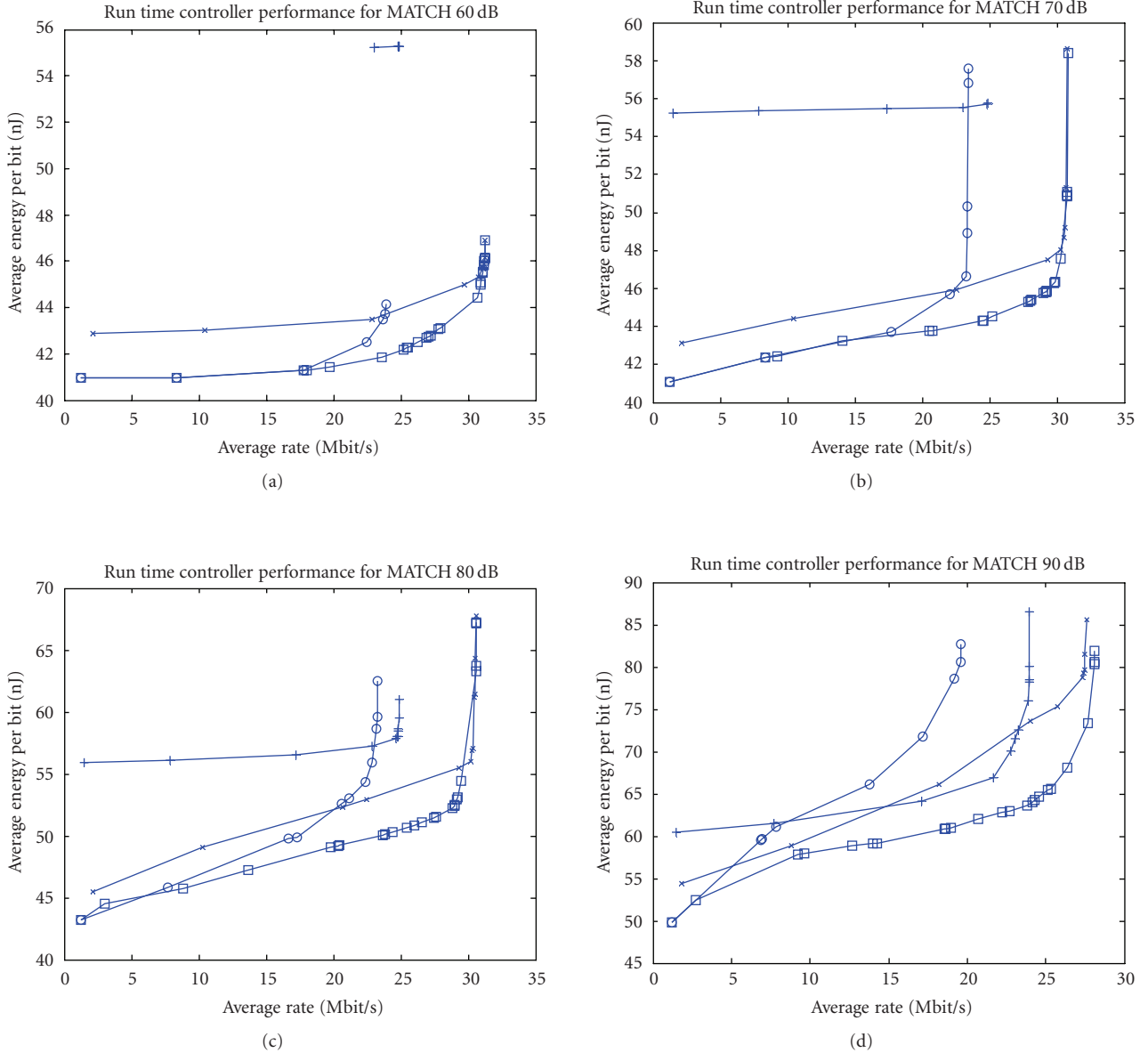


FIGURE 14: Average rate versus average energy-per-bit tradeoff for *smartMIMO* (bold line), superposed to the single-mode results. The energy efficiency is improved by up to 30% when compared to the single-mode results.

### 6.2. Average rate versus average energy-per-bit

By varying the average throughput constraint from 0 to the maximum achievable value ( $R_{\max}$ ), one can derive the set of extended control policies that lead to the Pareto optimal tradeoff between average throughput and average energy per bit. This tradeoff is depicted in Figure 14 for different path losses. The results of the multiantenna mode specific tradeoff curves are superposed for the sake of comparison.

Globally, it can be observed that the tradeoff achieved with the extended control policies always dominates the tradeoff achieved with the multiantenna mode-specific policies. An average power reduction up to 30% can be observed. The resulting throughput-energy tradeoff even dom-

inates SISO in the whole range, meaning that *smartMIMO* always brings a better energy per bit than any single mode. Moreover, this improvement does not affect the maximum throughput and range extension provided, respectively, by SDM and STBC. The energy benefit comes from a better adaptation to the channel conditions.

## 7. CONCLUSIONS

Multiantenna transmission techniques (MIMO) are being adopted in most broadband wireless standard to improve wireless links spectrum efficiency and/or robustness. There exists a well-documented tradeoff between potential spectrum efficiency and robustness increase. However, at



architecture level, multiantenna techniques also come with an overhead in power consumption due, at least, to the duplication of part of the transmitter and receiver radio front ends. Therefore, from a system perspective, it is the tradeoff between performance (e.g., the net throughput on top of the medium access control layer) and the average power consumption that really matters. It has been shown, in related works, that, in the case of narrow band single-carrier transceivers, adaptive schemes were mandatory to avoid that multiantenna techniques hamper this system-level tradeoff. In the broadband case, orthogonal frequency division multiplexing (OFDM) is usually associated with multiantenna processing. Adaptive schemes proposed so far for MIMO-OFDM optimize either the baseline physical layer throughput or the robustness in terms of bit-error rate. Energy efficiency is generally disregarded as well as the effects introduced by the medium access control (MAC) layer.

In this paper, the impact of adaptive SDM-OFDM and STBC-OFDM on the net data rate (on top of the MAC layer) versus energy-per-bit tradeoff has been analyzed and compared to adaptive SISO-OFDM. It has been shown that depending on the channel conditions, the one or the other scheme can lead to the best tradeoff. Up to a path loss of 80 dB, SISO always leads to the best energy efficiency up to a breakpoint rate (depending on the path loss) from where SDM is the most energy efficient. STBC improves the energy efficiency in a significant range of data rates only in case of large path loss (>90 dB).

Next, we derived and discussed *SmartMIMO*, an adaptive multiantenna scheme that controls, packet-per-packet, the basic OFDM links parameters (carrier modulation, forward error correction coding rate) as well as the type of multiple-antenna encoding (SISO, SDM, or STBC) in order to optimize the link net data rate (on top of the MAC) versus energy efficiency tradeoff. Based on a model calibrated on an existing multiantenna transceiver setup, the link energy efficiency with the proposed scheme is shown to be improved by up to 30% when compared to nonadaptive schemes. The average rate is, on the other hand, improved by up to 50% when compared to single-antenna transmission.

## ACKNOWLEDGMENTS

This work has been partially published in the Proceeding of the 20th IEEE Workshop on Signal Processing Systems (SiPS06) in October 2006. The project has been partially supported by Sony Corporation, the Samsung Advanced Institute of Technology (SAIT), and the Flemish Institute for BroadBand Telecommunication (IBBT, Ghent, Belgium). Bruno Bougard was Research Assistant delegated by the Belgian Foundation for Scientific Research (FWO) until October 2006.

## REFERENCES

- [1] A. B. Gershman, "Robust adaptive beamforming: an overview of recent trends and advances in the field," in *Proceedings of the 4th International Conference on Antenna Theory and Techniques (ICATT '03)*, vol. 1, pp. 30–35, Sevastopol, Ukraine, September 2003.
- [2] S. M. Alamouti, "A simple transmit diversity technique for wireless communications," *IEEE Journal on Selected Areas in Communications*, vol. 16, no. 8, pp. 1451–1458, 1998.
- [3] V. Tarokh, H. Jafarkhani, and A. R. Calderbank, "Space-time block codes from orthogonal designs," *IEEE Transactions on Information Theory*, vol. 45, no. 5, pp. 1456–1467, 1999.
- [4] G. J. Foschini, G. D. Golden, R. A. Valenzuela, and P. W. Wolniansky, "Simplified processing for high spectral efficiency wireless communication employing multi-element arrays," *IEEE Journal on Selected Areas in Communications*, vol. 17, no. 11, pp. 1841–1852, 1999.
- [5] L. Zheng and D. N. C. Tse, "Diversity and multiplexing: a fundamental tradeoff in multiple-antenna channels," *IEEE Transactions on Information Theory*, vol. 49, no. 5, pp. 1073–1096, 2003.
- [6] M. Zargari, D. K. Su, C. P. Yue, et al., "A 5-GHz CMOS transceiver for IEEE 802.11a wireless LAN systems," *IEEE Journal of Solid-State Circuits*, vol. 37, no. 12, pp. 1688–1694, 2002.
- [7] A. Behzad, L. Lin, Z. M. Shi, et al., "Direct-conversion CMOS transceiver with automatic frequency control for 802.11a wireless LANs," in *Proceedings of IEEE International Solid-State Circuits Conference (ISSCC '03)*, vol. 1, pp. 356–357, San Francisco, Calif, USA, February 2003.
- [8] B. Debaillie, B. Bougard, G. Lenoir, G. Vandersteen, and F. Catthoor, "Energy-scalable OFDM transmitter design and control," in *Proceedings of the IEEE 43rd Design Automation Conference (DAC '06)*, pp. 536–541, San Francisco, Calif, USA, July 2006.
- [9] C. Shuguang, A. J. Goldsmith, and A. Bahai, "Energy-constrained modulation optimization for coded systems," in *Proceedings of IEEE Global Telecommunications Conference (GLOBECOM '03)*, vol. 1, pp. 372–376, San Francisco, Calif, USA, December 2003.
- [10] W. Liu, X. Li, and M. Chen, "Energy efficiency of MIMO transmissions in wireless sensor networks with diversity and multiplexing gains," in *Proceedings of IEEE International Conference on Acoustics, Speech and Signal Processing (ICASSP '05)*, vol. 4, pp. 897–900, Philadelphia, Pa, USA, March 2005.
- [11] X. Li, M. Chen, and W. Liu, "Application of STBC-encoded cooperative transmissions in wireless sensor networks," *IEEE Signal Processing Letters*, vol. 12, no. 2, pp. 134–137, 2005.
- [12] R. W. Heath Jr. and A. J. Paulraj, "Switching between diversity and multiplexing in MIMO systems," *IEEE Transactions on Communications*, vol. 53, no. 6, pp. 962–972, 2005.
- [13] S. Catreux, V. Erceg, D. Gesbert, and R. W. Heath Jr., "Adaptive modulation and MIMO coding for broadband wireless data networks," *IEEE Communications Magazine*, vol. 40, no. 6, pp. 108–115, 2002.
- [14] M. H. Halmi and D. C. H. Tze, "Adaptive MIMO-OFDM combining space-time block codes and spatial multiplexing," in *Proceedings of the 8th IEEE International Symposium on Spread Spectrum Techniques and Applications (ISSSTA '04)*, pp. 444–448, Sydney, Australia, August 2004.
- [15] M. Codreanu, D. Tujkovic, and M. Latva-aho, "Adaptive MIMO-OFDM systems with estimated channel state information at TX side," in *Proceedings of IEEE International Conference on Communications (ICC '05)*, vol. 4, pp. 2645–2649, Seoul, Korea, May 2005.
- [16] P. Xia, S. Zhou, and G. B. Giannakis, "Adaptive MIMO-OFDM based on partial channel state information," *IEEE Transactions on Signal Processing*, vol. 52, no. 1, pp. 202–213, 2004.
- [17] B. Bougard, S. Pollin, A. Dejonghe, F. Catthoor, and W. Dehaene, "Cross-layer power management in wireless networks

- and consequences on system-level architecture,” *Signal Processing*, vol. 86, no. 8, pp. 1792–1803, 2006.
- [18] M. Wouters, T. Huybrechts, R. Huys, S. De Rore, S. Sanders, and E. Umans, “PICARD: platform concepts for prototyping and demonstration of high speed communication systems,” in *Proceedings of the 13th IEEE International Workshop on Rapid System Prototyping (IWRSP '02)*, pp. 166–170, Darmstadt, Germany, July 2002.
- [19] IEEE Std 802.11a, “Part 11: wireless LAN medium access control (MAC) and physical layer (PHY) specifications,” IEEE, 1999.
- [20] S. Valle, A. Poloni, and G. Villa, “802.11 TGn proposal for PHY abstraction in MAC simulators,” IEEE 802.11, 04/0184, February, 2004, <ftp://ieee:wireless@ftp.802wirelessworld.com/11/04/11-04-0184-00-000n-proposal-phy-abstraction-in-mac-simulators.doc>.
- [21] C. Schurgers, V. Raghunathan, and M. B. Srivastava, “Power management for energy-aware communication systems,” *ACM Transactions on Embedded Computing Systems*, vol. 2, no. 3, pp. 431–447, 2003.
- [22] V. Erceg, L. Schumacher, P. Kyritsi, et al., “TGn channel models,” Tech. Rep. IEEE 802.11-03/940r4, Wireless LANs, 2004.
- [23] K. M.iettinen, *Non-Linear Multi-Objective Optimization*, Kluwer Academic, Boston, Mass, USA, 1999.